MICROBUNCHING INSTABILITY IN RELATIVISTIC ELECTRON BUNCHES: DIRECT OBSERVATIONS OF THE MICROSTRUCTURES USING ULTRAFAST YBCO DETECTORS

E. Roussel, C. Evain, C. Szwaj, S. Bielawski, PhLAM/CERLA, Villeneuve d'Ascq, France
J. Raasch, P. Thoma, A. Scheuring, M. Hofherr, K. Ilin, S. Wünsch, M. Siegel
KIT, Karlsruhe, Germany
M. Hosaka, N. Yamamoto, and Y. Takashima, Nagoya University, Nagoya, Japan
H. Zen, Kyoto University, Kyoto, Japan
T. Konomi, M. Adachi, S. Kimura, M. Katoh, UVSOR, Okazaki, Japan

Abstract

Relativistic electron bunches circulating in accelerators are subjected to a dynamical instability leading to microstructures at millimeter to centimeter scale. Although this is a well-known fact, direct experimental observations of the structures, or the field that they emit, remained up to now an open problem. Here, we report the direct, shot-by-shot, time-resolved recording of the shapes (including envelope and carrier) of the pulses of coherent synchrotron radiation that are emitted, and that are a "signature" of the electron bunch microstructure. The experiments are performed on the UVSOR-III storage ring, using electrical field sensitive $YBa_2Cu_3O_{7-x}$ thin-film ultrafast detectors. The observed patterns are subjected to permanent drifts, that can be explained from a reasoning in phase space, using macroparticle simulations.

INTRODUCTION

Recent coherent synchrotron radiation (CSR) studies in storage rings have heightened the need for understanding the dynamics of electron bunches during the microbunching instability which is a source of intense emission of THz CSR pulses. This instability is known to lead to the formation of structures at millimeter scale in the longitudinal direction of the electron bunch [1]. However, direct observations of the dynamics of these microstructures were an open challenge up to now. Indeed, this requires to detect CSR pulses of hundreds or tens picoseconds length with internal structures at one to tens of picoseconds. Moreover, high-acquisition rate, typically of the order of tens of megahertz, would be required. Thus far, only indirect measurements were achieved by recording the spontaneously emitted coherent signal with slow detectors (at best with microsecond response time) [2–9] or by perturbating the electron bunch with an external laser [10, 11].

In this paper, we report on the first real time recordings of the pulse shape (envelope and carrier) associated with the CSR emitted during the microbunching instability when the electron bunch exceeds several tens of picoseconds [12]. The measurements have been obtained on the UVSOR-III storage ring [13] and have been possible through a new type of detector based on thin-film YBCO superconductor [14–16]. This detector has been developed at the Karlsruhe Institute of Technology (KIT) in Germany. We performed two types of experiments: the first one aims at studying the spontaneous emission of CSR during the microbunching instability; the second one aims at looking at the response of the electron bunch to a localized laser perturbation [2]. We describe the dynamics of CSR pulses from longitudinal phase-space motion.

EXPERIMENTAL SETUP

UVSOR-III Storage Ring

For the study of the spontaneous CSR emission, the UVSOR-III storage ring is operating in single bunch mode and the injected beam current is initially set above the instability threshold (here, around 53 mA). Under these conditions, the electron bunch emits CSR in the sub-terahertz frequency range which is a feature of the presence of longitudinal microstructures in the electron bunch at the millimeter scale. The CSR electric field (envelope and carrier) is detected through a new type of THz detector (YBCO, see next section for details) connected to an ultra-fast oscilloscope (63 GHz bandwidth, Agilent DSOX96204Q) at the BL6B infrared beamline [17](Fig. 1(a)).

A laser-electrons interaction in condition of slicing with picoseconds laser pulses is also possible and is achieved in the undulators U1 [18] (Fig. 1(b)). The beam current is just set below the instability threshold. The laser pulse is generated by an amplified Ti:Sa laser (Mira oscillator and Legend amplifier from Coherent) coupled with a cryogenic Ti:Sa amplifier (Legend Elite Cryo) which delivers a 800 nm, 10 mJ uncompressed laser pulses with a 300 ps duration at 1 kHz repetition rate. The pulses are compressed in the picoseconds range using an adjustable compressor with gratings [19]. Finally, the laser pulse is focused in the undulators U1 where it interacts with the electron bunch. The emitted coherent terahertz radiation is recorded at the BL6B infrared beamline using the YBCO detector and the same 63 GHz bandwidth oscilloscope.

YBCO Detector

The high-temperature superconductor $YBa_2Cu_3O_{7-x}$ (YBCO) is a new technology developed for the detection of radiation in the terahertz frequency range. The detector is composed of a YBCO superconducting thin-film detector

ISBN 978-3-95450-176-2

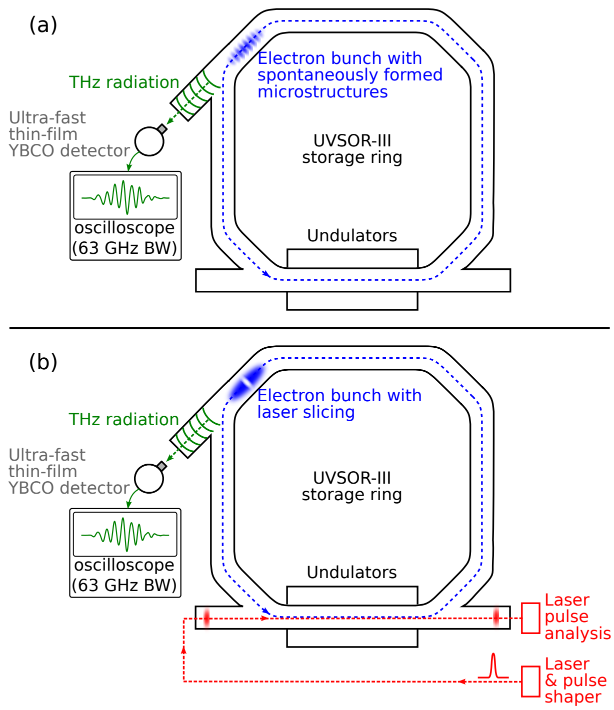

Figure 1: Experimental setups on the UVSOR-III storage ring. (a) Above a threshold beam current, an electron bunch undergoes an instability which leads to spontaneous formation of microstructures at the millimeter scale in the longitudinal direction. (b) Slicing experiment. A short laser pulse interacts with the electron bunch in the undulators U1. In both cases, the emission of coherent synchrotron radiation in the terahertz frequency range is recorded with the YBCO detector on the BL6B infrared beamline.

embedded in a broad-band THz antenna and cooled at liquid Nitrogen temperature and is designed for the analysis of CSR pulses [20].

The YBCO films are fabricated using the pulsed-laser deposition technique. A sapphire layer is used as substrate for the YBCO thin films because of its low dielectric losses which are essential for the back illumination of the YBCO detectors. The YBCO film is embedded between two buffer layers of PBCO ($PrBa_2Cu_3O_{7-x}$) to improve crystalline matching with the YBCO film. For YBCO film thickness above 30 nm, the critical temperature T_c is almost constant and well above the liquid nitrogen temperature of 77 K. To couple a broadband THz frequency range, a planar log-spiral antenna is implemented and embedded into a coplanar readout line. The coupling efficiency of the antenna in the 0.1 to 2 THz frequency range is higher than 90%. The sapphire substrates with antenna-coupled microbridges are glued to the rear, flat side of an elliptical silicon lens and mounted in a shielded holder to reduce interference with the electromagnetic fields at the beamlines.

Measurements at the MLS and ANKA storage rings revealed that the YBCO superconductor is a very sensitive and ultra-fast detector for radiation in the terahertz frequency range. Up to now, measurements achieved with the YBCO have highlighted a temporal resolution of 15 ps FWHM limited by the readout bandwidth (particularly by the 62.8 GHz bandwidth oscilloscope) [14]. They have also shown that the response of the YBCO detector used in zero-bias conditions is sensitive to the electric field of the radiation [14]. The photoresponse of YBCO films to picosecond CSR pulses is explained by direct interaction of vortices with the high-frequency electric field [15].

EXPERIMENTAL RESULTS

Spontaneous CSR Emission

Long-time series recorded at high resolution allow us to study the dynamics of the microbunching instability at different time scales as illustrated in Fig. 2. Therefore, the fast temporal resolution of the YBCO detector unveils the internal structures of the CSR pulse at tens of picosecond time scale. As can be seen in Fig. 2(c), the YBCO detector allows us to monitor the CSR electric field pulse, including the envelope and the optical carrier at $\approx$ 30 GHz. The CSR pulses have a duration of around 300 ps which is the same order of magnitude as the longitudinal electron bunch length. These CSR pulses are emitted periodically (Fig. 2(b)) with a repetition rate of 5.6 MHz (i.e. a period of 177 ns) which corresponds to the revolution frequency of a single bunch in the storage ring. At the millisecond time scale, slow dynamics of the coherent synchrotron radiation reveals that the emission occurs in a bursting manner far above the instability threshold (Fig. 2(a)). This dynamics is similar to what would be captured by a standard bolometer.

We summarized the dynamics of the CSR pulses as a color map versus a "fast time" (i.e., resolving the pulse shape), and a "slow time" (associated to the number of round-trips). The color map (Fig. 3) displays two features in the dynamics of the CSR pulses. The first one is the presence of structures at the head of the bunch(in the lower part of Fig. 3) which are drifting toward the tail of the electron bunch. The second one is the presence of an other structure which behaves erratically and drifts in both directions (localized around 200 ps in Fig. 3).

Laser-Slicing

The phase space dynamics can also be studied below the microbunching instability threshold, by examining the response to a perturbation to a short laser pulse that create a hole in the longitudinal electron bunch profile. Because the spontaneous microstructures are known to appear at the millimeter scale in the longitudinal direction of the electron bunch, the pulse duration of the perturbating laser is chosen in the tens to single picosecond range.

The experimental response presented in Fig. 4 is obtained using a 15 ps FWHM laser pulse.The perturbation is applied at time t = 0. An immediate response is visible just after the perturbation and a series of delayed response appears periodically with a period approximately equal to a half synchrotron period (at $\approx$ 25 µs, $\approx$ 50 µs). The data recorded by

ISBN 978-3-95450-176-2

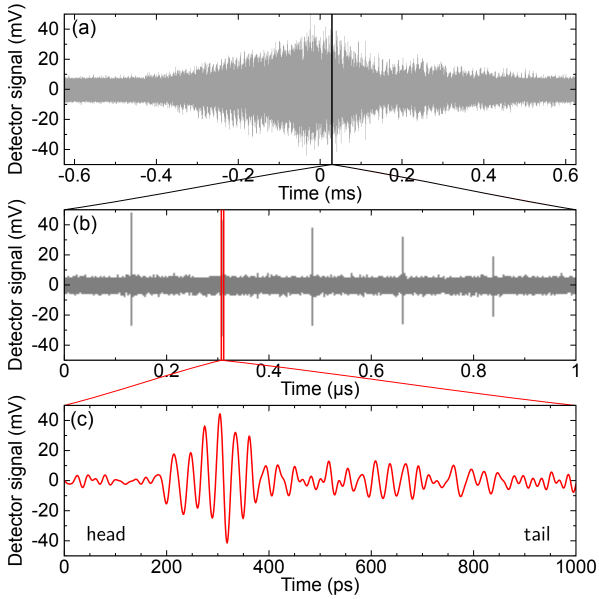

Figure 2: Terahertz CSR burst detected with the YBCO detector for a beam current I = 62 mA. (a) Slow variation of an entire CSR burst. The shape is similar to the traditional recordings with a bolometer or a Schottky diode except the alternating of positive and negative signal due to the sensitivity of the YBCO to electric field. (b) Zoom of (a) showing the CSR pulses emitted at each turn in the storage ring. (c) Zoom at one pulse in (b). The envelope and the carrier of the pulse are visible. The voltage of the detector signal is directly proportional to the incoming CSR electric field.

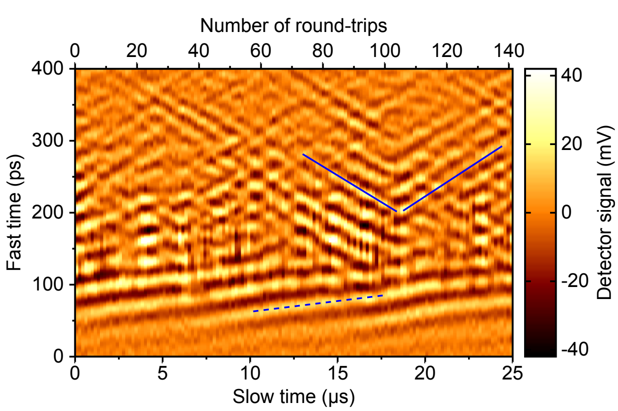

Figure 3: Color map representing the temporal evolution of the CSR electric field over many successive turns in the storage ring.

the YBCO detector display different characteristic features, as the arc shape at half synchrotron period (around ≈ 25 µs), and the cusp (or "Y shape) at the right of the color map.

NUMERICAL SIMULATIONS

The dynamics of the patterns observed in the CSR pulses can be interpreted from a reasoning in the longitudinal phase-

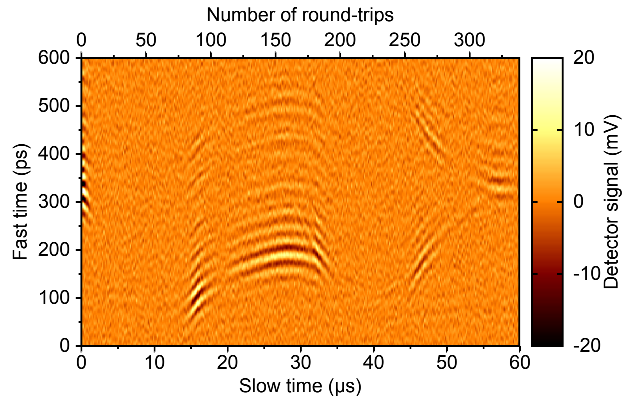

Figure 4: Dynamics following a localized laser perturbation (slicing) at $t = 0$, when the system is below the instability threshold. Note that no CSR emission is detected before $t < 0$.

space (longitudinal position z, energy E) of the electrons, assuming that the relevant motion occurs mainly in the longitudinal direction [21, 22]. For an accurate modeling of the dynamics, one needs to take into account collective effects inside the electron bunch, like, e.g. the shielded CSR impedance as well as the resistive and inductive impedances (see [23, 24] for a detailed description of the used model).

Spontaneous CSR Emission

The link between the electron phase-space distribution and the THz radiation recorded by the YBCO detector is illustrated in Fig. 5. Spontaneous formation of microstructures occurs in the electron bunch distribution $f(z, E, t)$ (Fig. 5(a)). However, only the projection on the z axis is observable, and corresponds to the longitudinal bunch profile $\rho(z, t) = \int_{-\infty}^{+\infty} f(z, E, t)dE$ (Fig. 5(b)). Even though the microstructures-induced modulations are extremely weak compared to the "global" shape of the electron bunch, they lead to a strong emission of CSR (Fig. 5(c)). We notice that the "spiral-shape" that wraps the whole bunch distribution is at the origin of the structures at the borders of the CSR pulse whereas the thin microstructures are responsible for the fast oscillations at the center. Because the electron bunch distribution rotates in phase-space, the structures in the CSR electric field drift along the longitudinal position, i.e. along the fast time axis (Fig. 5(d)). Thus, the structures drifting toward the tail (in the bottom part of Figs. 3 and 5(d)) are associated to the spiral while the structures moving in both directions are associated to the thin microstructures in the central part of the phase-sapce.

Laser-Slicing

A typical numerical simulation of the electron bunch response to a short laser perturbation is presented in Fig. 6. The laser perturbation is applied at time $t = 0$ µs. As in the experimental data (Fig. 4), we find a series of delayed response equally spaced, every half synchrotron period. The characteristic shapes of these responses can be understood

ISBN 978-3-95450-176-2

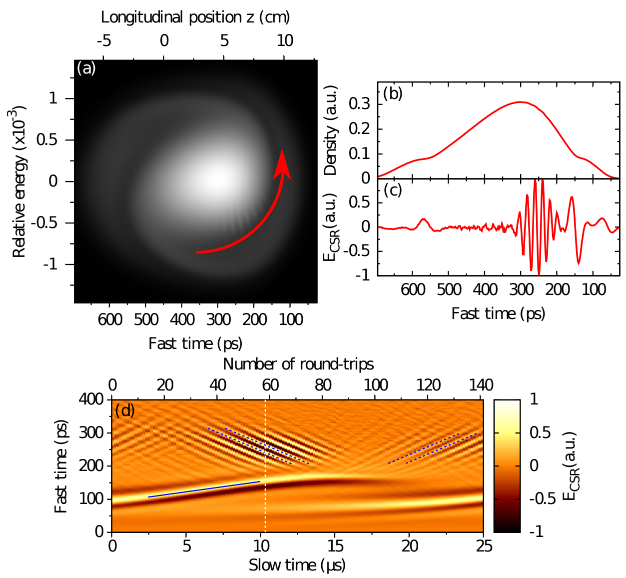

Figure 5: Interpretation of the drifting structures observed in Fig. 3, from numerical simulations. (a) Distribution of the electrons in longitudinal phase space (position z, energy E) at a given time. The CSR instability leads to a microstructure in this phase-space. (b) Longitudinal electron density distribution, i.e., obtained by the vertical projection of the distribution (a). (c) CSR electric field deduced from (b). Note that the structure is more visible in (c) than in (b), because the global shape of the electron bunch is cut off in the CSR process. The temporal evolution of the electric field (d) reveals that the structures are permanently drifting, as in the experiment. This is explained by the rotation of the electron distribution (a). (a,b,c) are taken at time $t = 10.4\,\mu s$ (white dashed line in (d)).

from the study of the phase-space versus time (Figs. 6(b-g)). Following the evolution of the slice, we can see that the Y-shape in Figs. 4 and 6(a) appears as a signature of the transformation of the initially straight slice (Fig. 6(c)) into an "S-shape" slice. The merging of the two branches of the cusp occurs when the inflexion point of the S-shape is almost vertical.

CONCLUSION

We have shown the first direct, real-time monitoring of the CSR pulses turn-by-turn. These experimental observations were possible using the detector based on ultra-fast thin-film YBCO superconductor which is sensitive to the electric field of the detected radiation. Thus, it is now possible to follow in detail the erratic behavior of CSR pulses, including envelope and carrier, in the millimeter wavelength range emitted during the microbunching instability. The detection method can also be extended to the detection of the envelope of pulses where the carrier cannot be resolved, by biasing the detector [16]. We also believe that the YBCO detector is a promising technology which will make it possible to test the validity of the existing or future models.

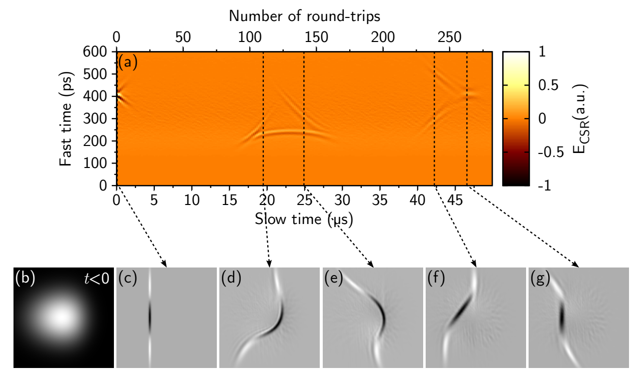

Figure 6: Numerical simulation of the electron bunch response to laser-slicing, and interpretation in phase space. (a) Color map of the temporal evolution of the CSR pulses. (b) Longitudinal electron bunch phase-space before laser-electrons interaction, (c,d,e,f,g) electron bunch distributions at different times after the laser perturbation. For clarity, the initial unperturbed electron distribution (a) has been subtracted.

ACKNOWLEDGMENT

The work was supported by the Joint Studies Program of the Institute for Molecular Science, the JSPS fellowship program for research in Japan (S-09171), the Projet International de Coopération Scientifique PICS project from CNRS, the Grant-in-aid for scientific researches (B20360041) of JSPS, the ANR (Blanc 2010-042301), and used HPC resources from GENCI TGCC/IDRIS (2013- x2013057057, 2014x2014057057). It has also been supported by Ministry of Higher Education and Research, Nord-Pas de Calais Regional Council and European Regional Development Fund (ERDF) through the Contrat de Projets État-Région (CPER) 20072013, and the LABEX CEMPI project (ANR-11-LABX-0007). The CERLA is supported by the French Ministère chargé de la Recherche, the Région Nord-Pas de Calais and the FEDER. The KIT is supported in part by the German Federal Ministry of Education and Research under Grant No. 05K2010.

REFERENCES

[1] M. Venturini *et al.*, Phys. Rev. ST Accel. Beams **8**, 014202 (2005)

[2] J. Byrd *et al.*, Phys. Rev. Lett. **89**, 224801(2002)

[3] V. Judin *et al.*, IPAC 2012, New Orleans, June 2012, TUPPP010 (2012)

[4] M. Abo-Bakr *et al.*, Phys. Rev. Lett. **88**, 254801 (2002)

[5] W. Shields *et al.*, Journal of Physics: Conference Series **357**, 012037 (2012)

[6] E. Karantzoulis *et al.*, Infrared Physics and Technology **53**, 300 (2010)

[7] G. Wüstefeld *et al.*, IPAC 2010, Kyoto, June 2010, WE-PEA015 (2010)

[8] C. Evain *et al.*, Europhys. Lett. **98**, 40006 (2012)

ISBN 978-3-95450-176-2

[9] A. Mochihashi *et al.*, EPAC06, Edinburgh, THPLS041 (2006)

[10] J. Byrd *et al.*, Phys. Rev. Lett. **97**, 074802 (2006)

[11] E. Roussel *et al.*, New Journal of Physics **16**, 063027 (2014)

[12] E. Roussel *et al.*, Phys. Rev. Lett. **113**, 094801 (2014)

[13] M. Adachi *et al.*, Journal of Physics: Conference Series **425**, 042013 (2013)

[14] P. Thoma *et al.*, Appl. Phys. Lett. **101**, 142601 (2012)

[15] P. Probst *et al.*, Phys. Rev. B **85**, 174511 (2012)

[16] P. Thoma *et al.*, IEEE Trans. Terahertz Sci. Technol. 3, 81 (2013)

[17] S. Kimura *et al.*, Infrared Physics and Technology **49**, 147-151 (2006)

[18] M. Adachi *et al.*, IPAC 2010, Kyoto, June 2010, WEPEA038 (2010)

[19] M. Hosaka *et al.*, Phys. Rev. ST Accel. Beams **16**, 020701 (2013)

[20] P. Thoma, Ph.D. thesis, Fakultät für Elektrotechnik und Informationstechnik, Karlsruher Institut für Technologie (KIT) (2013)

[21] M. Venturini and R. Warnock, Phys. Rev. Lett. **89**, 224802 (2002)

[22] G. Stupakov and S. Heifets, Phys. Rev. ST Accel. Beams **5**, 054402 (2002)

[23] E. Roussel *et al.*, IPAC 2014, Dresden, June 2014, TUPRI042 (2014)

[24] E. Roussel, Ph.D. thesis, Université Lille 1, Sciences et Technologie (2014)

ISBN 978-3-95450-176-2